# Interfacial Infrared Reflection Spectroscopic Evidence for Potential-Dependent Electrocatalytic Activity of Self-Assembled Monolayer of Nickel(II) Azamacrocyclic Complex toward Hydrogen Peroxide Oxidation

**K. Vengatajalabathy Gobi, Fusao Kitamura, Koichi Tokuda, and Takeo Ohsaka***

*Department of Electronic Chemistry, Interdisciplinary Graduate School of Science and Engineering, Tokyo Institute of Technology, 4259 Nagatsuta, Midori-ku, Yokohama 226-8502, Japan*

*Received: January 6, 1998; In Final Form: October 23, 1998*

Self-assembled monolayers (SAM) and mixed monolayers of a redox-active nickel(II) azamacrocyclic complex **1** show an efficient electrocatalytic activity toward the oxidation of $H_2O_2$. The cyclic voltammograms recorded at stationary and rotating disk electrodes for the electrocatalytic oxidation of $H_2O_2$ exhibit unique sharp anodic peaks of inverted "V" shape in both anodic and cathodic scans, largely depending on the concentration of the supporting electrolyte $NO_3^-$ anion. The electrocatalytic oxidation of $H_2O_2$ is found to proceed via an inner-sphere electron-transfer mechanism. The local concentration of $NO_3^-$ anions at the monolayer-solution interface is investigated in situ as a function of applied potential by subtractively normalized interfacial infrared reflection spectroscopy. The potential-dependent increase in the local concentration of $NO_3^-$ anion at the interface, which could lead to the stabilization of the intermediates involved in the electrocatalytic oxidation of $H_2O_2$, has been speculated as the cause for the unique cyclic voltammetric behavior observed in the electrocatalytic oxidation of $H_2O_2$.

## Introduction

Modification of gold surfaces with organosulfur compounds offers highly organized, stable, and compact self-assembled monolayers (SAMs) because of the covalent S−Au bonding.[1] SAMs have been studied intensively to develop molecular electronic devices, thin-film optics, protecting layers, electrochemical sensors, etc. SAMs possessing redox-active functional groups are also interesting for studying the long-range electron-transfer kinetics under a well-defined chemical environment, for developing molecular sensors, etc.[2−7] The influences of solvent reorganization, ion transport, etc. at the monolayer-solution interface on heterogeneous electron-transfer kinetics of redox-active SAMs have been demonstrated recently.[8−10] In particular, a detailed knowledge of the monolayer-solution interface, for example, on the molecular orientation and ion distribution, is an essential prerequisite for understanding mediated electron transfer and electrocatalytic reactions at a redox-active SAM. In the present investigation, electrocatalytic oxidation of $H_2O_2$ at SAM and mixed-monolayers of **1**, dinickel-

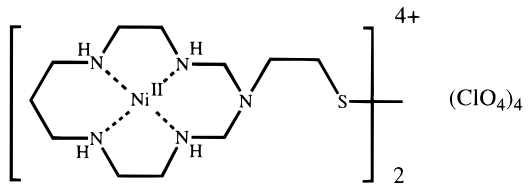


**1**

(II) (2,2-bis(1,3,5,8,12-pentaazacyclotetradec-3-yl)-diethyl disulfide) perchlorate, was studied. The unique potential-dependent electrocatalytic phenomena observed have been successfully explained on the basis of SNIFTIR (subtractively normalized interfacial Fourier transform infrared) spectroscopic measurements of the SAM−electrolyte solution interface.

## Experimental Section

The dinickel complex **1** was synthesized according to our procedure reported elsewhere.[11] Complex **1** was characterized by elemental analysis, $^{13}C$ NMR, and IR spectral measurements. Diethyl disulfide, $NaNO_3$, and $H_2O_2$ were of Analar grade (Kanto Chemical, Japan). Deionized water (Milli-Q system, Millipore, Japan) was used to prepare electrolyte solutions.

Polycrystalline gold electrodes of 1 mm (voltammetry) and 10 mm (SNIFTIR spectroscopy) diameters were polished with aqueous slurries of successively finer alumina powder (down to 0.06 $\mu$m) and were sonicated for 10 min in water. Electrodes were cleaned in 0.05 M $H_2SO_4$ by potential cycling in the range −0.2 to 1.5 V.[12] The real surface area was calculated from the charge required to reduce the surface oxide layer.[13] The SAM of **1** was fabricated by soaking the Au electrodes thus pretreated into methanol solution of 0.5 mM **1** for at least 36 h; mixed monolayers of **1** were constructed from methanol solutions containing different mole fractions of **1** and diethyl disulfide at a total disulfide concentration of 0.5 mM.

Electrochemical measurements were performed with a BAS 100 B/W electrochemical analyzer. The working and the Pt counter electrodes were separated by a porous glass. An NaCl saturated Ag/AgCl electrode was used as the reference electrode. For rotating disk voltammetry, a rotary system from Nikko Keisoku Co., Japan was employed. SNIFTIR spectra were recorded with a Bio-Rad Laboratories FTS-7T FTIR spectrometer equipped with a liquid-$N_2$-cooled HgCdTe detector. The resolution of the system was 8 $cm^{-1}$. For each spectrum, 640 interferograms were collected to achieve a good signal-to-noise ratio. P-polarized light was used throughout the measurements

* To whom correspondence should be addressed. Fax: +81-45-924-5489. E-mail: ohsaka@echem.titech.ac.jp.

10.1021/jp980634g CCC: $18.00 
Published on Web 12/11/1998

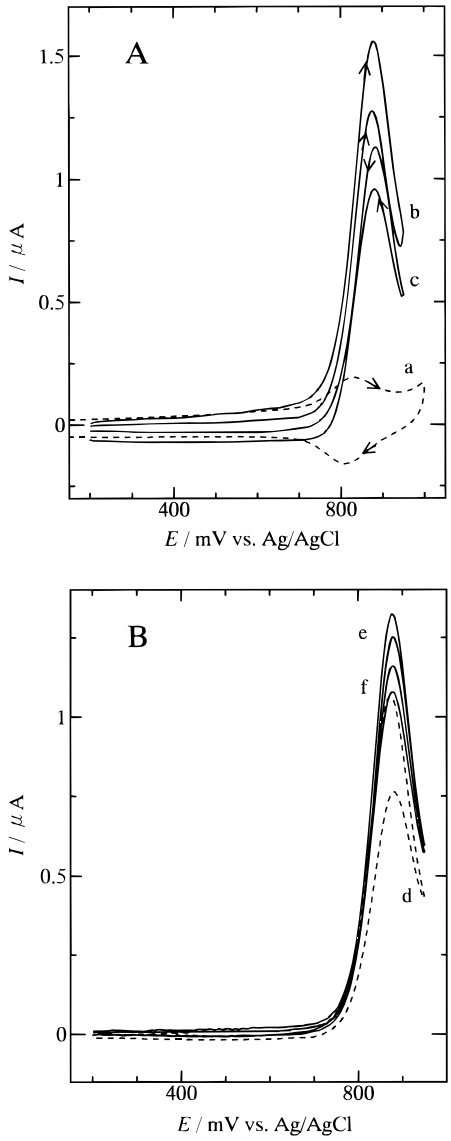


**Figure 1.** (A) CVs of the SAM of **1** ($1.45 \times 10^{-10}$ mol cm$^{-2}$) in aqueous solutions (pH 2.7) of 0.1 M $NaNO_3$ in the absence (a) and presence (b−f) of 1 mM $H_2O_2$. (B) CVs of the SAM of **1** on stationary (dotted line) and rotating disk (solid line) electrodes. Rotation rates are 900 (e) and 400 (f) rpm. Potential scan rates were 100 (a,b), 20 (c), and 10 (d−f) mV s$^{-1}$.

by utilizing a wire grid polarizer. The incident angle of IR radiation at the air−$CaF_2$ window was ca. 60°. Electrolyte solutions were deaerated by bubbling $N_2$ gas for at least 30 min prior to electrochemical and IR spectral measurements.

## Results and Discussion

**Electrochemical Measurements. 1** was shown to self-assemble on a gold surface to yield a monolayer of nickel(II) complex.[14] The cyclic voltammograms (CVs) of the SAM of **1** in an aqueous 0.1 M $NaNO_3$ (pH 2.7) solution in the presence and absence of 1 mM $H_2O_2$ are shown in Figure 1A. In the absence of $H_2O_2$, a symmetrical reversible redox wave was obtained at 0.82 V and the $\Delta E_p$ value, although not zero, was typically very small. The CV of the SAM of **1** (curve a of Figure 1A) is consistent in all respects with that anticipated for an electrochemically reversible reaction involving a surface-confined species. The surface coverage (Γ) of nickel(II) redox centers, $1.45 \times 10^{-10}$ mol cm$^{-2}$, was obtained from the graphical integration of the anodic wave and corresponds to a square close-packed monolayer of nickel(II) redox centers on the gold surface.[14,15] The monolayer of **1** was found to be stable on potential cycling for the $Ni^{2+/3+}$ redox process, and 90% of the electroactivity (based on the anodic peak charge $Q_p^a$) of **1** remained after 10 potential cycles for the $Ni^{2+/3+}$ redox process at a scan rate of 100 mV s$^{-1}$.

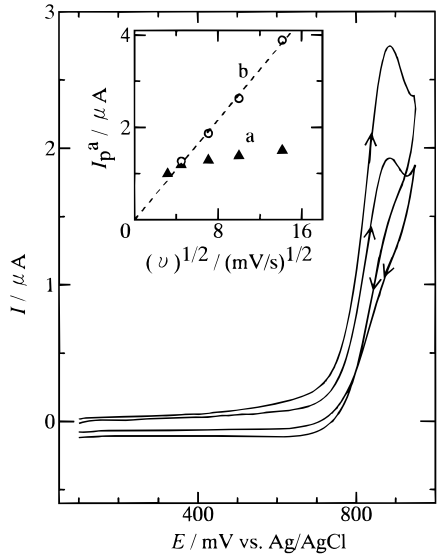


**Figure 2.** CVs of the SAM of **1** in a solution (pH 2.7) of 10 mM $NaNO_3$ and 1 mM $H_2O_2$. Potential scan rates were 100 and 50 mV s$^{-1}$. Inset shows the dependence of $I_p^a$ on $\upsilon^{1/2}$. The CVs were collected in solutions of 0.1 M (a) and 10 mM (b) $NaNO_3$ containing 1 mM $H_2O_2$.

On addition of 1 mM $H_2O_2$, the anodic peak current ($I_p^a$) increased enormously with the disappearance of the cathodic peak (curve b of Figure 1A). The $I_p^a$ for the electrocatalytic oxidation of $H_2O_2$ remained constant for a set of few potential cycles at a scan rate of 100 mV s$^{-1}$. It shows that the monolayer of nickel complex is stable during the electrocatalysis of $H_2O_2$ oxidation. The $I_p^a$ for the electrocatalytic oxidation of $H_2O_2$ does not scale linearly with the square root of scan rate, $\upsilon^{1/2}$ (Figure 2 (inset)); therefore, the observed $I_p^a$ values are not diffusion-controlled but catalytic reaction-controlled. The anodic peak potential, $E_p^a$, of the electrocatalytic oxidation of $H_2O_2$ (0.87 V) is found to be more positive than that of the nickel(II) complex (0.83 V) in the self-assembly (Figure 1A). This shows that the oxidation of $H_2O_2$ by the electroproduced nickel(III) complex might be a process involving intermediates. Moreover, in an aqueous solution of 1 M $NaNO_3$, CVs were recorded for the SAM of **1** in the presence and absence of $H_2O_2$ and are shown in Figure 3. In the absence of $H_2O_2$, a reversible redox wave for the $Ni^{2+/3+}$ redox couple of the SAM of **1** was observed (curves a′ and b′ of Figure 3). But in the presence of $H_2O_2$, the CV recorded at 500 mV s$^{-1}$ (Figure 3a) shows an additional peak (*) at more positive potentials; at slow scan rates, only the more positive peak is observed (Figure 3b). These facts suggest that the electrocatalytic oxidation of $H_2O_2$ by the SAM of **1** is not a simple electron cross-exchange reaction but would be a process involving intermediates; i.e., the electrooxidation of Ni(II) complex to Ni(III) complex occurs at the prewave, and the intermediate(s) forming between the nickel(III) complex and $H_2O_2$ undergoes electrooxidation in the more positive potential region (*; Figure 3a). The $I_p$ and $Q_p$ values of the $Ni^{2+/3+}$ redox process were independent of the concentration of $NaNO_3$, 0.1 and 1 M, at a given $\upsilon$. But *the $I_p^a$ for the electrocatalytic oxidation of $H_2O_2$ in aqueous 1 M $NaNO_3$ is low relative to that in aqueous 0.1 M $NaNO_3$* (Figures 3 and 1A). Since solvent molecules/anions are known to coordinate

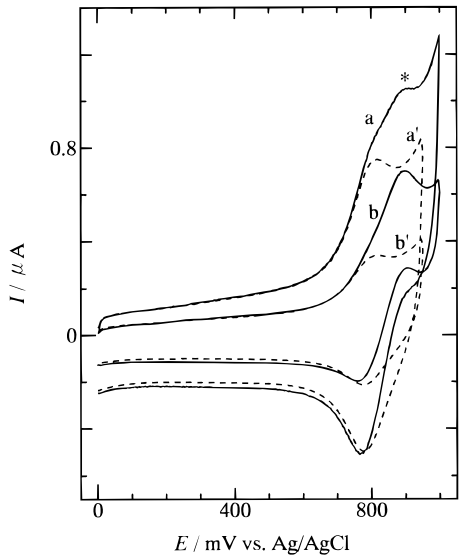


**Figure 3.** CVs of the SAM of **1** in a solution of 1 M $NaNO_3$ (pH 2.7) in the absence (dotted curves) and presence (solid curves) of 2 mM $H_2O_2$. Potential scan rates were 500 (a,a′) and 200 (b,b′) mV $s^{-1}$.

to the nickel(III) complex through the axial positions,[11,16−18] the observed results for the electrocatalytic oxidation of $H_2O_2$ could be associated with an inner-sphere electron-transfer mechanism rather than an outer-sphere one. *The CVs of the SAM of **1** in the presence of $H_2O_2$ display sharp anodic peaks of inverted "V" shape in both anodic and cathodic scans* (Figure 1A). Generally, the CV for an electrocatalytic oxidation mediated by surface-immobilized species shows an anodic peak in the anodic scan without any anodic current in the reverse scan;[19] but at the SAM of **1**, the electrocatalytic oxidation of $H_2O_2$ showed sharp anodic peaks in both anodic and cathodic scans. So *the observed electrocatalysis could be a potential-dependent process but not a conventional redox state-dependent process.* The electrocatalytic oxidation of $H_2O_2$ was also pursued at mixed-monolayers of **1** and diethyl disulfide with different $\Gamma$ values of **1** ($0.82 \times 10^{-10}$ and $0.56 \times 10^{-10}$ mol $cm^{-2}$). We observed a similar unique cyclic voltammetric behavior for the electrocatalytic oxidation of $H_2O_2$, together with a decrease in $I_p^a$ with decreasing $\Gamma$ of **1**. The unique cyclic voltammetric behavior is expected to reflect the mechanistic details of the electrocatalytic oxidation of $H_2O_2$ by the SAM of **1**.

Figure 1B shows the CVs of the SAM of **1** on a gold rotating disk electrode (RDE). At the RDE also, the CVs for the oxidation of $H_2O_2$ show sharp anodic peaks of inverted "V" shape in both anodic and cathodic scans. Generally, current response for an electrocatalytic oxidation at RDEs using surface-immobilized species shows an S-shaped curve with a plateau current, which is purely controlled by the mass transport of substrate molecules.[19] But we observed sharp anodic peaks in both anodic and cathodic scans at the SAM of **1**. *This observation establishes that the electrocatalytic activity of the nickel(III) complex of the SAM of **1** toward $H_2O_2$ oxidation is dependent on the applied electrode potential and clearly indicates that the transport of substrate molecules, $H_2O_2$, to the electrode surface is not the cause for the observed unique cyclic voltammetric behavior. Consequently, the observed unique behavior would have been caused by a potential-dependent process involving surface-immobilized species at monolayer-solution interface during the electrocatalytic oxidation of $H_2O_2$ at the SAM of **1***. The electrocatalytic activity of the SAM of **1** was found to be almost retained in continuous potential cycles. On continuous potential cycling at RDEs, the $I_p^a$ for the electrocatalysis of $H_2O_2$ oxidation decreased by only a very small extent (~5%) in the second scan at a potential scan rate of 10 mV $s^{-1}$ and an electrode rotation rate of 400 rpm. Recently, Lever and co-workers observed very similar unique CVs, possessing cathodic peaks in both the cathodic and anodic scans, for the electrocatalytic reduction of sodium nitrite at a glassy carbon (GC) electrode adsorbed with iron−alizarin complexone.[20] At RDE (rotation rate of 400 rpm), the cathodic peak observed in the anodic scan disappeared; an unknown product of the nitrite reduction is speculated as the cause for their observations.[20]

The electrocatalytic oxidation of $H_2O_2$ at the SAM of **1** was carried out in aqueous 10 mM $NaNO_3$ containing 1 mM $H_2O_2$ (Figure 2). At reduced concentrations of $NaNO_3$, 10 mM, the CVs of the SAM of **1** recorded in the presence of $H_2O_2$ show increased anodic peak currents compared with the case of 0.1 M $NaNO_3$ (see curve b of Figure 1A and Figure 2 at 100 mV $s^{-1}$). The shape of the observed CVs appears to be that of a simple diffusion-controlled process, and in fact, the $I_p^a$ scales linearly with $v^{1/2}$ (Figure 2 (inset)). The electrocatalytic oxidation of $H_2O_2$ in 0.01, 0.1, and 1 M $NaNO_3$ solutions clearly suggests that the $NO_3^-$ anions significantly take part in the rate-determining step of the catalytic oxidation process of $H_2O_2$ by the SAM of **1**.

Recently, Jiang and Dong also observed[21] similar unique CVs, possessing anodic peaks in both anodic and cathodic scans, for the electrocatalytic oxidation of $H_2O_2$ at a cobalt protoporphyrin modified pyrolytic graphite electrode. The cobalt(III) protoporphyrin, the oxidizing redox mediator, is expected to form a relatively more stable Lewis acid−base complex with $O_2$, the product of electrocatalysis, than the cobalt(II) protoporphyrin. Hence, the inner-sphere electrocatalytic oxidation of $H_2O_2$ by the cobalt(III) protoporphyrin could be slowed by the formation of a stable acid−base complex between cobalt(III) redox center and $O_2$. Thus, the $I_p^a$ for the electrocatalysis is decreased at more positive potentials, where more and more stable complexes between cobalt(III) protoporphyrin and electroproduced $O_2$ could be formed.[21] But in the present case, the CVs of Figure 2 showed a simple diffusion-controlled behavior, with increased anodic peak currents, in the other way, with high yields of $O_2$. Moreover, both in oxygenated and deaerated solutions containing 10 mM $NaNO_3$ (pH 2.7) and 1 mM $H_2O_2$, the CVs of the SAM of **1** showed a voltammetric behavior expected for a totally diffusion-controlled reaction, and the anodic peak currents for electrocatalysis at a given $v$ are equal (not shown). These observations thus clearly rule out the formation of a stable complex between $O_2$ and the nickel(III) complex.

According to the experimental results, the electrocatalytic oxidation of $H_2O_2$ by the SAM of **1** is suggested to take place as shown in Scheme 1. Since nickel(III) complexes are of octahedral geometry with axially coordinated solvent molecules/anions,[11,16−18] the electroproduced nickel(III) complex of the SAM of **1** is considered to undergo an equilibrium with the nitrate-coordinated intermediate A. Since the electrocatalytic oxidation of $H_2O_2$ by the SAM of **1** is an inner-sphere electron-transfer process (vide supra), the intermediate B is formed in the presence of $H_2O_2$ by the substitution of $NO_3^-$ anion by $H_2O_2$ in the intermediate A or directly from the uncoordinated nickel(III) complex. Intramolecular electron transfer from the hydroperoxide anion to the nickel(III) metal center leads to the formation of "C". Further heterogeneous electron-transfer and intramolecular electron-transfer and deprotonation produce $O_2$ with the regeneration of the nickel(II) complex. According to the Scheme 1, the change in the $I_p^a$ for the electrocatalytic

**SCHEME 1: Probable Reaction Mechanism for the Electrocatalytic Oxidation of $H_2O_2$ by the SAM of 1 in Aqueous Solutions of $NO_3^-$ Anion[a]**

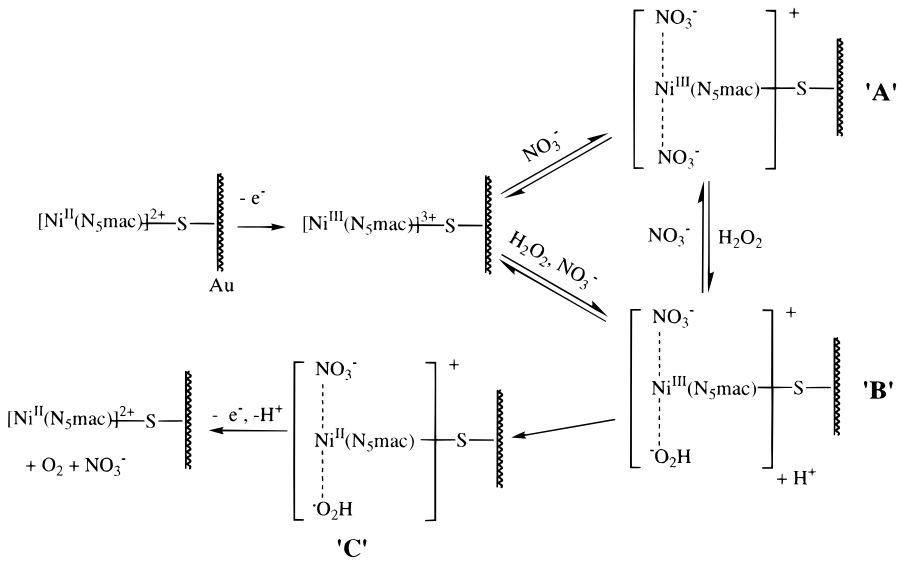


[a] $N_5$mac and $^{\bullet}O_2H$ represent the pentaaza macrocycle of complex **1** and the hydroxyl radical, respectively.

oxidation of $H_2O_2$ at the SAM of **1** (Figures 1−3) with 0.01, 0.1, and 1 M of $NaNO_3$ could be explained. High concentrations of $NaNO_3$ lead to the formation of more and more nitrate-coordinated intermediate A and to the stabilization of intermediate A over intermediate B. The stabilization of "A" and the shift in the equilibrium between "A" and "B" toward "A" could slow the electrocatalytic oxidation of $H_2O_2$ by the SAM of **1**. At a suitably low concentration of $NaNO_3$ (10 mM), the intermediates A and B seem to be not as stabilized so that all the substrate molecules, $H_2O_2$, diffusing to the monolayer-solution interface quickly undergo electrocatalytic oxidation to give a diffusion-controlled current (Figure 2 (inset)). Though the reaction mechanism in Scheme 1 could explain the variation of $I_p$[a] for electrocatalytic oxidation of $H_2O_2$ at different concentrations of $NaNO_3$ (Figure 2 (inset)), the observation of the "inverted" anodic peak in the cathodic scan would not be explicable; *i.e., the potential-dependent electrocatalytic activity of the SAM of **1** could not be explained by a scheme of chemical reactions. Thus, apart from the chemical reactions described in Scheme 1, a potential-dependent process involving surface-immobilized species is also presumed to control the electrocatalytic oxidation of $H_2O_2$.* In the following section, a probable explanation for the sharp anodic peaks of inverted "V" shape observed in both anodic and cathodic scans will be given on the basis of the SNIFTIR spectroscopic measurements of the SAM−electrolyte solution interface.

**Spectral Measurements.** Figure 4A shows the SNIFTIR spectra of the SAM of **1** on a polycrystalline Au electrode recorded in aqueous 0.1 M $NaNO_3$ (pH 2) at different sampling potentials, $E_s$. A reference potential, $E_r$, of 0.2 V, where no faradic process takes place, was used. The $E_s$ was changed stepwise from 0.4 V, where no faradic process of $Ni^{2+/3+}$ of SAM of **1** occurs, to 0.95 V, and the spectra obtained in the region 1000−2000 $cm^{-1}$ were examined to understand the structure and composition of $NO_3^-$ anions at the SAM−electrolyte solution interface. At the $E_s$ of 0.7 V, a new negative-going band appears in the region 1300−1400 $cm^{-1}$ and monotonically increases as the $E_s$ becomes more and more positive (Figure 4A). In reflection spectroscopy, note that the negative and positive signs of bands indicate an increase and decrease, respectively, in absorption intensity at the respective sampling potential; an increase in the absorption intensity is attributed to an increase in the concentration of the corresponding IR-active species. At $E_s = 0.85$ V, where the nickel complex of the SAM of **1** is almost completely oxidized in its trivalent state, a well-developed negative-going band was seen at ∼1370 $cm^{-1}$, which could be assigned to the NO stretching mode of $NO_3^-$ anions solvated in aqueous solutions.[22] The NO stretching mode of $NO_3^-$ anions coordinated to the nickel(III) complex is expected to appear at 1305 and 1420 $cm^{-1}$.[22] Further changes in $E_s$ to 0.9 and 0.95 V surprisingly led to an enormous increase in the intensity of the band at 1370 $cm^{-1}$. These observations suggest that the increase in the effective concentration of $NO_3^-$ anions at the interface is not only due to the coordination of $NO_3^-$ anions to the nickel(III) complex but also to other phenomena, for example, their adsorption/accumulation at the monolayer-solution interface (vide infra).

Figure 4B shows the plot of peak height of the band at 1370 $cm^{-1}$ against the $E_s$. At potentials more positive than 0.85 V, the peak height increased steeply, implying that the effective concentration of the $NO_3^-$ anion increases enormously at the SAM−electrolyte solution interface at potentials more positive than 0.85 V.

Figure 5 shows a set of SNIFTIR spectra obtained at a bare Au electrode in an aqueous solution of 0.1 M $NaNO_3$ (pH 2). As the $E_s$ becomes more positive, a negative-going band grows at ∼1370 $cm^{-1}$. Relative to the SAM of **1**, the spectral data of the bare Au electrode differ significantly in the following ways: (a) at the SAM of **1** the band at 1370 $cm^{-1}$ appears at $E_s = 0.7$ V and more positive potentials, while at the bare Au electrode the corresponding band is visible at $E_s$ as low as 0.5 V; (b) the intensity of the negative-going band at the SAM of **1** is higher than that at the bare Au electrode; (c) at the SAM of **1**, the intensity of the band largely grows with an increase in $E_s$ once it started to appear at $E_s = 0.7$ V. The negative-going band at 1370 $cm^{-1}$ seems to respond to the potential of zero charge (pzc) of the Au electrode. The reference potential of 0.2 V vs Ag/AgCl is close to the pzc.[23,24] At potentials more positive than the pzc, the electrode surface is charged positively. The observed results show that more $NO_3^-$ anions either adsorb on the electrode surface or come close to the electrode−solution interface as the $E_s$ becomes more positive than the pzc. Recently, Watanabe and co-workers studied the adsorption of anions ($ClO_4^-$ and $HSO_4^-$) on a polycrystalline gold surface by using

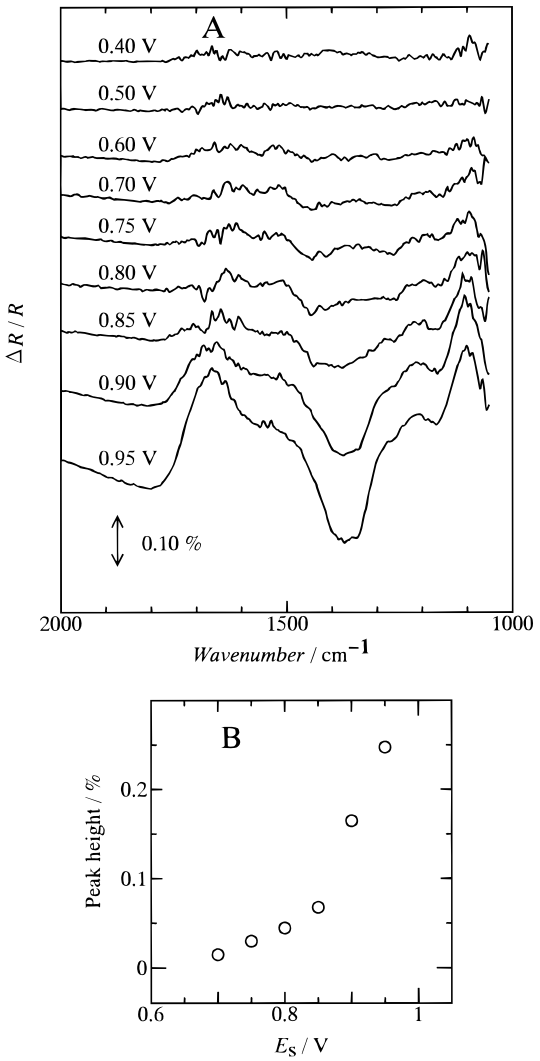


**Figure 4.** (A) SNIFTIR spectra of the SAM of **1** on a gold electrode in a solution of 0.1 M $NaNO_3$ (pH 2) as a function of $E_s$ (indicated on each spectrum). The reference potential was 0.2 V. (B) Plot of peak height against $E_s$.

EQCM[25] at potentials more positive than the pzc and found that anions of as much as $\sim 5.8 \times 10^{-10}$ mol $cm^{-2}$ adsorb on the electrode surface. From the relative intensities of the negative-going band (at 1370 $cm^{-1}$) at the SAM of **1** and at the bare Au electrode (Figures 4 and 5), the number of $NO_3^-$ anions at the monolayer-solution interface is considered to be larger than that at the bare Au electrode−solution interface.

From the SNIFTIR spectral investigations of the SAM of **1** and bare Au electrode, the local concentration of $NO_3^-$ anions near the SAM−electrolyte solution interface is found to increase enormously with increasing electrode potential in the region 0.85−0.95 V (Figure 4B) because of the coordination of $NO_3^-$ anions with surface-immobilized nickel(III) complex and because of the attraction of $NO_3^-$ anions by a positively charged gold surface, at the potentials more positive than the pzc. The nitrate anions coordinating with the nickel(III) complex of the SAM of **1** can be expected to have different orientations with respect to the electrode surface because of their free rotation along the axis of coordination; similarly, the nitrate anions accumulating at the interface could not be in a single specific orientation with respect to the electrode surface. According to the IR surface selection rules,[26] the $NO_3^-$ anions having a transition dipole moment parallel to the electrode surface are IR-inactive and any $NO_3^-$ anions having a transition dipole moment not parallel to the electrode surface are IR-active. Thus, the real concentration of $NO_3^-$ anions at the interface might be higher than that expected from the SNIFTIR spectral studies. Increase in the local concentration of $NO_3^-$ anions will lead to favorable formation of more and more of the nitrate anion-coordinated intermediate A.

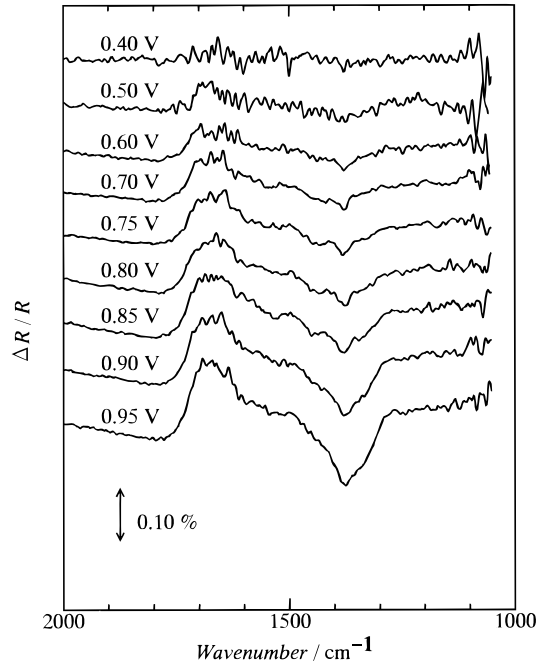


**Figure 5.** SNIFTIR spectra at bare Au electrode in 0.1 M $NaNO_3$ as a function of $E_s$. Other conditions are the same as those in Figure 4A.

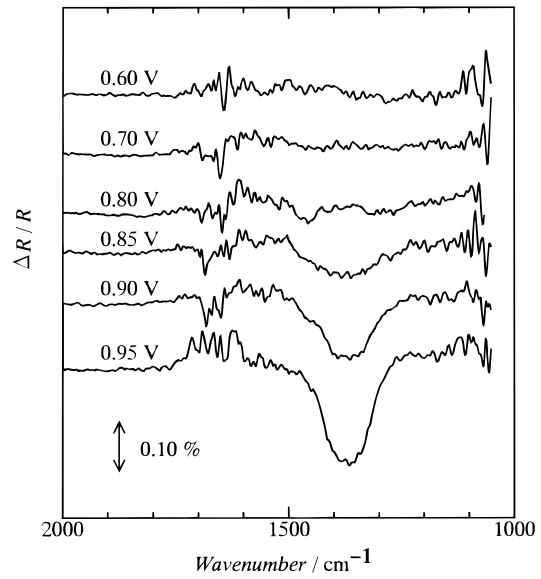


**Figure 6.** SNIFTIR spectra of the SAM of **1** on a gold electrode in aqueous 0.1 M $NaNO_3$ (pH 2) containing 1 mM $H_2O_2$ as a function of $E_s$. The reference potential was 0.2 V.

The interface of the SAM of **1** was also probed in the presence of $H_2O_2$. As observed in the absence of $H_2O_2$, the negative-going band at $\sim$1370 $cm^{-1}$ appears also in the presence of $H_2O_2$ (Figure 6). Since the IR vibrations of $H_2O_2$, $\sim$3360 $cm^{-1}$,[27] will coincide with those of bulk water, $\sim$3450 $cm^{-1}$,[22] and since the cutoff region of the $CaF_2$ window falls in the region 1050−600 $cm^{-1}$, where prominent IR vibrations, 635 and 878 $cm^{-1}$,[27] of $H_2O_2$ are present, the IR vibrations of peroxide were not observed in the SNIFTIR spectral measurements.[27,28] The band at 1370 $cm^{-1}$ becomes visible only from 0.8 V and increases

enormously in the region 0.85−0.95 V (Figure 6). In the presence of $H_2O_2$ also, the effective concentration of $NO_3^-$ anions at the interface increases enormously, which could lead to the formation of more and more $NO_3^-$-coordinated intermediates, A, and to the stabilization of intermediate A over the intermediate B. *The stabilization of intermediate A and the shift in the equilibrium between "A" and "B" toward "A" could slow the electrocatalytic oxidation of $H_2O_2$ by the nickel(III) complex.* Such a potential-dependent increase in the local concentration of $NO_3^-$ anions near the SAM−electrolyte solution interface could lead to a potential-dependent change in the electrocatalytic current for the oxidation of $H_2O_2$, at potentials more positive than 0.85 V, as seen in Figures 1 and 3. *In the cathodic scan from 0.95 V, the concentration of $NO_3^-$ anions at the interface starts to decrease, resulting in an increase in the anodic current for the electrocatalytic oxidation of $H_2O_2$.* On the other hand, in the case of electrolyte solutions containing 10 mM $NaNO_3$, the potential-dependent increase in the local concentration of $NO_3^-$ anions might not be enough to provide an effective stabilization of intermediate A.

**Acknowledgment.** The present work was financially supported by Grant-in-Aids for Scientific Research on Priority Areas of "New Polymers and Their Nano-Organized Systems" (No. 277/10126219), "Exploratory Research" (No.09875207), and "Scientific Research (A)" (No.10305064) from the Ministry of Education, Science, Sports and Culture, Japan and the Katoh Science Foundation, Japan. K.V.G. acknowledges the Government of Japan for Monbusho Fellowship. The authors acknowledge the comments and suggestions made by the reviewers.

## References and Notes

(1) (a) Finklea, H. O. In *Electroanalytical Chemistry*; Bard, A. J., Rubinstein, I., Eds.; Marcel Dekker: New York, 1996; Vol. 19, p 109. (b) Dubois, L. H.; Nuzzo, R. G. *Annu. Rev. Phys. Chem.* **1992**, *43*, 437.

(2) Finklea, H. O.; Hanshew, D. D. *J. Am. Chem. Soc.* **1992**, *114*, 3173.

(3) Tender, L.; Carter, M. T.; Murray, R. W. *Anal. Chem.* **1994,** *66*, 3173.

(4) Acevedo, D.; Abruna, H. D. *J. Phys. Chem.* **1991**, *95*, 9590.

(5) Sato, Y.; Fujita, M.; Mizutani, F.; Uosaki, K. *J. Electroanal. Chem.* **1996**, *409*, 145.

(6) Zak, J.; Yuan, H.; Ho, M.; Woo, L. K.; Porter, M. D. *Langmuir* **1993**, *9*, 2772.

(7) Hutchison, J. E.; Postelthwaite, T. A.; Murray, R. W. *Langmuir* **1993**, *9*, 3227.

(8) Smith, C. P.; White, H. S. *Anal. Chem.* **1992**, *64*, 2398.

(9) Redepenning, J.; Tunison, H. M.; Finklea, H. O. *Langmuir* **1993**, *9*, 1404.

(10) Forster, R. J.; Faulkner, L. R. *J. Am. Chem. Soc.* **1994**, *116*, 5453.

(11) Gobi, K. V.; Ohsaka, T. *Electrochim. Acta* **1998**, *44*, 269.

(12) Ataka, K.; Yotsuyanagi, T.; Osawa, M. *J. Phys. Chem.* **1996**, *100*, 10664.

(13) Gileadi, E.; Eisner, K. E.; Penciner, J. *Interfacial Electrochemistry—An Experimental Approach*; Addison-Wesley: Reading, MA, 1975.

(14) Gobi, K. V.; Okajima, T.; Tokuda, K.; Ohsaka, T. *Langmuir* **1998**, *14*, 1108.

(15) (a) Fabbrizzi, L.; Lanfredi, A. M. M.; Pallavicini, P.; Perotti, A.; Taglietti, A.; Ugozzoli, F. *J. Chem. Soc., Dalton Trans.* **1991**, 3263. (b) Ducharme, D.; Salesse, C.; Leblanc, R. M.; Meller, P.; Mertesdorf, C.; Ringsdorf, H. *Langmuir* **1993**, *9*, 2145.

(16) (a) Lappin, A. G.; McAuley, A. *Adv. Inorg. Chem.* **1988**, *32*, 241. (b) Haines, R. I.; McAuley, A. *Coord. Chem. Rev.* **1981**, *39*, 77.

(17) Lovecchio, F. V.; Gore, E. S.; Busch, D. H. *J. Am. Chem. Soc.* **1974**, *96*, 3109.

(18) (a) Zeigerson, E.; Bar, I.; Bernstein, J.; Kirschenbaum, L. J.; Meyerstein, D. *Inorg. Chem.* **1982**, *21*, 73. (b) Zilbermann, I.; Meshulam, A.; Cohen, H.; Meyerstein, D. *Inorg. Chim. Acta* **1993**, *206*, 127.

(19) Bard, A. J.; Faulkner, L. R. *Electrochemical Methods—Fundamentals and Applications*; John Wiley: New York, 1980.

(20) Zhang, J.; Lever, A. B. P.; Pietro, W. J. *Inorg. Chem.* **1994**, *33*, 1392.

(21) Jiang, R.; Dong, S. *J. Electroanal. Chem.* **1990**, *291*, 11.

(22) Nakamoto, K. *Infrared and Raman Spectra of Inorganic and Coordination Compounds*, 4th ed.; Wiley-Interscience: New York, 1986.

(23) Lipkowski, J.; Ross, P. N. *Structure of Electrified Interfaces*; VCH: New York, 1993.

(24) Chen, J. H.; Nie, L. H.; Yao, S. Z. *J. Electroanal. Chem.* **1996**, *414*, 53.

(25) Uchida, H.; Ikeda, N.; Watanabe, M. *J. Electroanal. Chem.* **1997**, *424*, 5 and references therein.

(26) Stole, S. M.; Popenoe, D. D.; Porter, M. D. In *Electrochemical Interface: Modern Techniques for In-situ Interface Characterization*; Abruna, H. D., Ed.; VCH: New York, 1991; p 339.

(27) Taylor, R. C. *J. Chem. Phys.* **1950**, *18*, 898.

(28) The frequency of the promising IR band of $H_2O_2$, ∼1350 $cm^{-1}$, is close to that of the $NO_3^-$ anion.[22,27] But the intensity of the negative-going band at 1350 $cm^{-1}$ at the SAM of **1** is not higher in the presence of $H_2O_2$ than that in the absence; i.e., we could not detect the coordinated $H_2O_2$. This could be attributed to the efficient electrocatalytic activity of the SAM of **1** toward $H_2O_2$ oxidation; because of the efficient electrocatalytic activity, the hydroperoxide anions coordinating with the nickel(III) complex will have only a transition time at the interface. Hence, the detection of peroxide coordinated to the nickel(III) redox center could become difficult.